

The effect of water on the hydrogenation of *o*-chloronitrobenzene in ethanol, *n*-heptane and compressed carbon dioxide



Haiyang Cheng^{a,b}, Xiangchun Meng^c, Yancun Yu^{a,b}, Fengyu Zhao^{a,b,*}

^a State Key Laboratory of Electroanalytical Chemistry, Changchun Institute of Applied Chemistry, Chinese Academy of Sciences, Changchun 130022, PR China

^b Laboratory of Green Chemistry and Process, Changchun Institute of Applied Chemistry, Chinese Academy of Sciences, Changchun 130022, PR China

^c School of Chemical Engineering, Changchun University of Technology, Changchun 130012, PR China

ARTICLE INFO

Article history:

Received 12 December 2012

Received in revised form 17 January 2013

Accepted 20 January 2013

Available online 9 February 2013

Keywords:

o-chloronitrobenzene

Hydrogenation

Water

Compressed carbon dioxide

ABSTRACT

Water as a clean solvent and promoter in the organic synthesis have attracted more attention, herein the effect of water was studied for the hydrogenation of *o*-chloronitrobenzene (*o*-CNB) over Pt/C and Pd/C catalysts in ethanol, *n*-heptane and compressed CO₂. Very interesting, the reaction rate decreased in ethanol, but increased in *n*-heptane and compressed CO₂ with the addition of water. The role of water in the reaction was mainly discussed from the experimental data and phase behavior analysis, one is to activate the functional group of NO₂ through the interactions via a hydrogen bonding, and the other is to affect the solubility of hydrogen in ethanol and *n*-heptane. The positive effect of the interaction between water and reactants may be counteracted by the negative effect of hydrogen solubility in ethanol. However, the concentration of *o*-CNB and hydrogen changed slightly in *n*-heptane with the addition of water, so the interaction of water with reactants may play a main role in improving the TOF. The combination of H₂O and CO₂ is more efficient than the pure H₂O, CO₂ and H₂O–*n*-heptane systems. The phase behavior may play important role also for the improved activity except for the interactions of H₂O and CO₂ with the reactants. *o*-CNB phase was expanded in the compressed CO₂ and so the concentration of H₂ in *o*-CNB phase increased due to the miscible of CO₂ and H₂, resulting in the enhancement of reaction rate and the maximum conversion at pressure of 9 MPa CO₂, at which the volume was expanded to the largest one. The similar results were also obtained in the compressed CO₂ system without H₂O. In addition, the stability of Pt/C and Pd/C was studied in H₂O–*n*-heptane and H₂O–CO₂. As a result, the H₂O–CO₂ media and Pt/C catalyst is one of the most effective systems for the hydrogenation of *o*-CNB.

© 2013 Elsevier B.V. All rights reserved.

1. Introduction

Water is the most abundant, cheap, safe and environmental friendly solvent in nature and the study of organic reactions in aqueous solvents is an important theme of current research [1–3]. High reaction rate and product selectivity was reported to be obtained in some organic reactions in pure water [4–10], particularly for some cases of the organic reactants are insoluble in the aqueous phase (“on water”) [2,11–16]. In addition, the use of water as solvent has the common advantages including simple separation of organic product and safe operation owing to its high heat capacity and unique redox stability. In the hydrogenation of nitroaromatics, the positive effect of water has been reported

in literature [17–23], for example, water addition remarkably promotes the selective hydrogenation of CNB in ethanol over SiO₂ supported Ru, Fe, Co, Ni, Cu and Ag catalysts [21], and Ru/MgF₂ [22] and Ir/ZrO₂·xH₂O [23]. In contrast, the presence of more than 10% of water in ethanol slowed down the rate of nitrobenzene hydrogenation over Pt/Pt₂O as reported by Adams et al. [24]. Recently, Laniri et al. reported that the activities in water were greater than those in a biphasic medium consisting of water and toluene (1:1) in the hydrogenation of CNBs over a water-soluble polymer protected platinum carbonyl cluster [16]. The effects of H₂O are contradictory in the hydrogenation of nitroaromatics and the reasons are still unclear.

Supercritical carbon dioxide (scCO₂) is an attractive environmentally benign reaction medium in comparison with conventional organic solvents, due to its nonflammability, relative inertness, complete miscibility with gases, and easy separation from liquid/solid products [25,26]. Furthermore, scCO₂ can show interesting effects on reaction rates and product selectivity [26–39], which was ascribed to the interaction of compressed CO₂ with reacting species (i.e., nitrobenzene, nitrosobenzene, and

* Corresponding author at: State Key Laboratory of Electroanalytical Chemistry, Changchun Institute of Applied Chemistry, Chinese Academy of Sciences, 5625 Renmin Street, Changchun, Jilin 130022, PR China. Tel.: +86 431 8526 2410; fax: +86 431 8526 2410.

E-mail address: zhaofy@ciac.jl.cn (F. Zhao).

N-phenylhydroxylamine) [27–29] and modification of the catalyst surface with CO generated from CO₂ hydrogenation [35]. Compared with pure scCO₂ or H₂O solvent, the combination of CO₂ and H₂O is more beneficial for selective hydrogenation of water-insoluble organic compounds [29,32,40–42]. Recently, the present authors had studied the hydrogenation of nitrobenzene (NB) and CNB over supported Ni catalysts in H₂O–CO₂. We found the reaction rate was higher in H₂O–CO₂ than those in H₂O or scCO₂, and the selectivity to aniline and chloroaniline (CAN) reached about 100% in the whole range of conversion for the reactions in H₂O–CO₂ and scCO₂ [29]. However, the deactivation of catalyst was serious, especially in H₂O–CO₂.

In present work, we studied the effect of water on the hydrogenation of *o*-CNB over Pt/C and Pd/C in ethanol, *n*-heptane and compressed CO₂. In addition, the effect of CO₂ pressure on the conversion and selectivity was also studied and discussed in detail, and the results difference to the previous Ni/TiO₂ catalyst was discussed from the phase behavior and the catalyst hydrophilic properties. The Pt/C catalyst was demonstrated to be effective and stable for the hydrogenation of *o*-CNB in H₂O–CO₂.

2. Experimental

2.1. Chemicals

5 wt% Pd/C and 5 wt% Pt/C catalysts were purchased from WAKO and used as received. Ethanol, *n*-heptane and *o*-CNB from Beijing Chemical Reagent Cooperation, are of analytical grade and used without further purification. The water was deionized water. Gases of H₂ (99.999%), N₂ (99.999%) and CO₂ (99.999%) were used as delivered.

2.2. Catalyst characterization

The average size of Pd and Pt crystalline particles was estimated by X-ray diffraction (XRD) pattern recorded on D8 ADVANCE X-ray Diffractometer, and calculated by the Debye–Scherrer formula. X-ray photoelectron spectroscopy (XPS, VG Microtech 3000 Multilab) was used to examine the electronic properties of Pt and Pd on the surface of the Pt/C and Pd/C catalysts. The C 1s peak at 284.6 eV arising from adventitious carbon was used as reference. This reference gives binding energy values with a precision of ±0.2 eV. The surface composition of the samples was determined from the peak areas of the corresponding lines using a Shirley type background and empirical cross section factors for XPS. The fresh catalysts were characterized directly. The used catalysts, prior to characterization, were washed thoroughly with ethanol for 6 times, separated by centrifugation, and dried in vacuum at 60 °C overnight. The leaching of Pt and Pd into solvents was measured by ICP-OES (iCAP6300, Thermo USA).

2.3. Hydrogenation reaction

The hydrogenation of *o*-CNB was carried out in a 50 ml high-pressure stainless steel batch reactor. In a typical experiment, catalyst (5 mg), *o*-CNB (1.5 g) and deionized water (10 ml) were loaded into the reactor. Then the reactor was sealed and flushed three times with N₂ to remove air, and heated to the reaction temperature of 35 °C. Hydrogen (4 MPa) and then liquid CO₂ was introduced into the reactor using a high-pressure liquid pump to the desired pressure. The reaction mixture was stirred continuously with a magnetic stirrer during reaction. The stirring speed was 1200 rpm to make sure that the reaction was free from any significant mass transport limitations. After reaction the reactor was cooled in ice-water bath, depressurized carefully, and the liquid product was extracted with *n*-hexane/diethyl ether (*v/v* = 1/1)

and analyzed with a gas chromatograph (GC-Shimadzu-2010, FID, Capillary column, Rtx-5 30 m × 0.25 mm × 0.25 μm), and identified by gas chromatography/mass spectrometry (GC/MS, Agilent 5890, FID, Capillary column, HP 5). The GC results were obtained using an internal standard method and biphenyl was always used as internal standard. Hydrogenation reactions in H₂O, scCO₂, *n*-heptane, H₂O–*n*-heptane, ethanol and H₂O–ethanol were conducted in the same reactor using similar procedures. For recycling experiment in H₂O–*n*-heptane, the reaction mixture of the first run was separated by decantation, and then the solid catalysts were washed three times with *n*-heptane and reused. The next run was started with the fresh *o*-CNB and *n*-heptane. For recycling experiment in H₂O–CO₂, the reaction mixture of the first run was extracted by scCO₂, and the solid catalyst and water were reused for the next run with adding fresh *o*-CNB, and reaction was started under the similar conditions.

2.4. Visual observation of the phase behavior in H₂O–CO₂

The observation of the phase state of *o*-CNB in H₂O–CO₂ was carried out in an 85 ml high-pressure view cell. Water (17 ml) and *o*-CNB (2.55 g) were added and the reactor was heated up to 35 °C, H₂ (4 MPa) and then liquid CO₂ was introduced into the reactor to the required pressure. At each pressure the mixture was stirred for several minutes, and then the stirring was stopped and the phase behavior was observed by the naked eye through the transparent sapphire windows.

3. Results and discussion

3.1. Catalytic performances of Pd/C and Pt/C in different reaction media

Table 1 shows the results of hydrogenation of *o*-CNB over Pd/C in different reaction systems. The turnover frequency (TOF) in ethanol (28.5 s⁻¹) was much higher than that in H₂O (11.0 s⁻¹) (entries 1, 6), but it was lowered down (17.2 s⁻¹) by introducing water (entry 7). The selectivity to *o*-CAN was <90% in ethanol and H₂O–ethanol due to the dechlorination and the accumulation of intermediates (*o*-chloronitrosobenzene (CNSB), *N*-chloro-phenylhydroxylamine (CPHA), dichloroazoxybenzene (CAOB), dichloroazobenzene (CAB), and dichlorohydrazobenzene (CHAB)) (entries 6–10). In H₂O, it reached to 98.6% and did not change much with extending reaction time at complete conversion (entries 4, 5). The TOF in *n*-heptane (9.79 s⁻¹) was slightly lower than that in H₂O (11.0 s⁻¹) (entries 1, 11), but it was enhanced to 15.3 s⁻¹ by introducing water into *n*-heptane (entry 12), and further enhanced by introducing less amount of water into *n*-heptane (entry 13, 14). In H₂O–*n*-heptane, the selectivity to *o*-CAN reached to 99.5% at complete conversion of *o*-CNB and did not change much with extending reaction time because the dechlorination and the accumulation of intermediates was low in a conversion range of 50–100% (entries 14–17). The TOF in 9 MPa CO₂ (4.3 s⁻¹) was lower than that in H₂O (11.0 s⁻¹) (entries 1, 18), but it was improved (19.9 s⁻¹) in the H₂O–9 MPa CO₂ system (entry 23). The time needed for a complete conversion in H₂O–CO₂ (65 min) was much short than that in H₂O (120 min) and scCO₂ (360 min) (entry 3, 20, 25). At complete conversion, the selectivity to *o*-CAN in H₂O–CO₂ (99%) was higher than that in H₂O (98.5%) and scCO₂ (95.5%) (entries 5, 22, 25), due to that the dechlorination and the accumulation of intermediates (CNSB, AOB, AB, and HAB) were fully inhibited in H₂O–CO₂, and it did not change much with extending reaction time (entry 26).

For Pt/C catalyst (Table 2), the TOF in ethanol (87.3 s⁻¹) was much higher than that in H₂O (6.95 s⁻¹) (entries 1, 2), but it was slightly decreased to 85.4 s⁻¹ by introducing water into ethanol

Table 1
Hydrogenation of *o*-CNB over 5% Pd/C in various media.

Entry	Medium	Time (min)	Conversion (%)	Selectivity (%)			TOF ^a (s ⁻¹)	
				<i>o</i> -CAN	Dechlo. ^b	Others ^c		
1	10 ml H ₂ O	25	28	87.8	1.4	10.8	11.0	
2		60	55	89.3	1.2	9.5	8.96	
3		120	99	96.5	1.2	2.3	8.07	
4		180	100	98.6	1.2	0.2	–	
5		260	100	98.5	1.5	–	–	
6	10 ml ethanol	25	73	78.7	3.9	17.4	28.5	
7	2 ml H ₂ O + 8 ml ethanol	25	44	70.7	6.1	23.2	17.2	
8		60	99	78.8	5.9	15.3	16.1	
9	9 MPa CO ₂	120	100	86.9	7.2	5.9	–	
10		180	100	88.4	11.0	0.6	–	
11		25	25	95.0	0.5	4.5	9.79	
12		10 ml H ₂ O + 10 ml <i>n</i> -heptane	25	39	94.5	0.8	4.7	15.3
13		6 ml H ₂ O + 10 ml <i>n</i> -heptane	25	45	95.2	0.8	4.0	17.6
14		2 ml H ₂ O + 10 ml <i>n</i> -heptane	25	50	97.4	0.7	1.9	19.6
15		65	98	98.9	0.5	0.6	14.7	
16	10 ml H ₂ O + 9 MPa CO ₂	120	100	99.5	0.5	–	–	
17		180	100	99.3	0.7	–	–	
18		25	11	86.0	2.0	12.0	4.30	
19		240	81	76.2	0.2	23.6	3.30	
20		360	99	89.9	0.6	9.5	2.69	
21		480	100	92.5	0.5	7.0	–	
22	10 ml H ₂ O + 9 MPa CO ₂	600	100	95.5	0.6	3.9	–	
23		25	51	94.1	1.2	4.7	19.9	
24		50	92	96.8	0.6	2.6	18.0	
25		65	100	99.0	0.7	0.3	–	
26		120	100	99.0	1.0	–	–	

Reaction conditions: 5 mg 5% Pd/C, 9.52 mmol *o*-CNB, 4 MPa H₂, 35 °C.

^a Turnover frequency; which was given as the overall rate of *o*-CNB conversion normalized by the number of active sites over the specified time. The number of active sites was calculated by (the metal dispersion) × (the total number of supported metal atoms). The Pd dispersion (*D*) was calculated from the following equation: Dispersion = $6(\nu_m/a_m)/d$, where ν_m and a_m are equal to 14.70 Å³ and 7.93 Å², respectively, and the average diameter (*d*) of Pd particles was determined to be 16.1 nm by XRD measurements.

^b By-products from dechlorination are aniline and nitrobenzene.

^c Intermediates include *o*-chloronitrosobenzene, dichloroazoxybenzene, dichloroazobenzene, and dichlorohydrazobenzene.

(entry 3). The TOF in *n*-heptane (41.7 s⁻¹) was much higher than that in H₂O (6.95 s⁻¹) (entries 1, 4), and it was slightly enhanced (42.7 s⁻¹) by introducing water into *n*-heptane (entry 6). The selectivity to *o*-CAN in H₂O-*n*-heptane was higher than that in *n*-heptane

at complete conversion of *o*-CNB (entries 5, 7). The TOF in 9 MPa CO₂ (34.4 s⁻¹) was much higher than that in H₂O (6.95 s⁻¹) (entries 1, 8), and was further enhanced (45.0 s⁻¹) in the H₂O-9 MPa CO₂ system (entry 14). The conversion and selectivity to *o*-CAN increased

Table 2
Hydrogenation of *o*-CNB over 5% Pt/C in various media.

Entry	Medium	Time (min)	Conversion (%)	Selectivity (%)			TOF ^a (s ⁻¹)
				<i>o</i> -CAN	Dechlo. ^b	Others ^c	
1	10 ml H ₂ O	25	35	81.4	1.2	17.4	6.95
2	10 ml ethanol	5	88	70.6	0.8	28.6	87.3
3	2 ml H ₂ O + 8 ml ethanol	5	86	61.6	0.9	37.5	85.4
4	10 ml <i>n</i> -heptane	5	42	79.1	1.6	19.3	41.7
5	10 ml H ₂ O + 10 ml <i>n</i> -heptane	25	100	91.5	2.2	6.3	–
6		5	43	83.5	0.4	17.2	42.7
7	9 MPa CO ₂	25	100	96.2	0.5	3.3	–
8		7.5	52	61.8	0.3	37.9	34.4
9		15	87	68.0	0.5	31.5	28.8
10		25	99	74.0	0.6	25.4	19.7
11		60	100	80.8	0.6	18.6	–
12		180	100	90.6	0.3	9.1	–
13		300	100	99.0	0.6	0.4	–
14	10 ml H ₂ O + 9 MPa CO ₂	7.5	68	62.8	0.2	37.0	45.0
15	10 ml H ₂ O + 9 MPa CO ₂	15	95	61.6	0.1	38.3	31.4
16		25	100	69.7	0.1	30.2	–
17		120	100	83.7	0.2	16.1	–
18		240	100	97.5	0.3	2.2	–
19		300	100	99.5	0.3	0.2	–

Reaction conditions: 5 mg 5% Pt/C, 9.52 mmol *o*-CNB, 4 MPa H₂, 35 °C.

^a Turnover frequency; which was given as the overall rate of *o*-CNB conversion normalized by the number of active sites over the specified time. The number of active sites was calculated by (the metal dispersion) × (the total number of supported metal atoms). The Pt dispersion (*D*) was calculated from the following equation: Dispersion = $6(\nu_m/a_m)/d$, where ν_m and a_m are equal to 15.10 Å³ and 8.07 Å² respectively, and the average diameter (*d*) of Pt particles was determined to be 4.5 nm by XRD measurements.

^b By-products from dechlorination are aniline and nitrobenzene.

^c Intermediates include *o*-chloronitrosobenzene, dichloroazoxybenzene, dichloroazobenzene, and dichlorohydrazobenzene.

with extending reaction time, and the selectivity to dechlorination byproducts was lower than 0.6% in 9 MPa CO₂ and H₂O–CO₂ (entries 8–19); the selectivity to *o*-CAN reached to 99.0% in 9 MPa CO₂ and 99.5% in H₂O–CO₂ at complete conversion of *o*-CNB (entries 13, 19).

The addition of 20% water to ethanol had negative effect on the conversion of *o*-CNB over Pd/C and Pt/C catalysts, although water, ethanol and *o*-CNB are miscible and catalyst was uniformly dispersed in the mixture under the conditions. The effect of water may be considered from the following two factors (a) the interactions of water with the reacting species (i.e., *o*-CNB, *o*-CNSB, and CPHA) and (b) solubility of hydrogen and *o*-CNB in the solution. It was reported that hydrogen bonds were formed intermolecular of NB and H₂O that protrude farthest into the organic phase through molecular dynamics study of the H₂O/NB interface [43,44]. The N–O bond of PHA is weakened through interaction with H₂O as confirmed by FTIR results [29], possibly via OH...O and OH...N bonding [45]. These interactions may also exist between *o*-CNB, *o*-CNSB, *o*-CHPA and H₂O, and could be favorable to the hydrogenation of –NO₂, –NO and –NHOH groups. The solubility of hydrogen changed with the composition of H₂O–ethanol and it decreased markedly with increase of water volume in ethanol. For example, the solubility of hydrogen decreased about 40% when 20% of water was introduced into ethanol [17]. When increase of both the amount of catalyst and the water content, the rate determining step may change from the surface catalytic reaction to the mass transfer of hydrogen [17]. Herein, for Pd/C and Pt/C catalyst, the solubility of hydrogen in the solvent may play the main role in controlling the reaction rate. The positive effect of the interaction between H₂O and reactants may be counteracted by the negative effect of hydrogen solubility with increasing water content in ethanol.

Laniri et al. reported that the activities in H₂O were greater than those in a biphasic medium consisting of H₂O and toluene (1:1) in the hydrogenation of CNBs over water-soluble polymer protected platinum carbonyl cluster, owing to that the catalyst was dispersed in aqueous phase and the concentrations of dissolved CNBs in the aqueous phase in pure H₂O were higher than those in H₂O–toluene biphasic medium [16]. However, in the present results, over Pd/C and Pt/C, the activity in *n*-heptane and H₂O was lower than that in a biphasic medium consisting of H₂O and *n*-heptane (1:1). Pd/C and Pt/C were hydrophobic and mainly dispersed in *n*-heptane, and the concentrations of *o*-CNB and hydrogen in *n*-heptane did not change much, so the interactions of H₂O with the reacting species should play an important role in the improved TOF in H₂O–*n*-heptane. The activity in 9 MPa CO₂ and H₂O was also lower than that in H₂O–9 MPa CO₂ biphasic medium, which may be due to the interactions of H₂O and CO₂ with the reacting species, and will be described in detail below.

3.2. Influence of CO₂ pressure and phase behavior

Biphasic system especially H₂O–CO₂ medium is more effective for the selective hydrogenation of *o*-CNB and inhibits the dechlorination. CO₂ pressure exerted a significant effect on the conversion, as shown in Fig. 1. In the H₂O–CO₂ system, with CO₂ pressure up to 9 MPa, the conversion increased from 45% to 92% for Pd/C and increased from 23% to 95% for Pt/C catalysts, but it decreased with the further increasing of CO₂ pressure (Fig. 1a, b). In the compressed CO₂ system, with CO₂ pressure up to 9 MPa, the conversion increased from 43% to 87% for Pt/C catalyst, and it decreased also with the further increasing of CO₂ pressure (Fig. 1c).

The phase behavior, and the concentration of *o*-CNB and hydrogen in the liquid and CO₂ phases might be important factors in determining the rate of *o*-CNB hydrogenation. Under the reaction conditions, as shown in Fig. 2, three phases of gas CO₂, H₂ and dissolved *o*-CNB, liquid *o*-CNB (*o*-CNB, dissolved H₂ and CO₂) and liquid H₂O presented at the CO₂ pressure below 17.4 MPa, and then

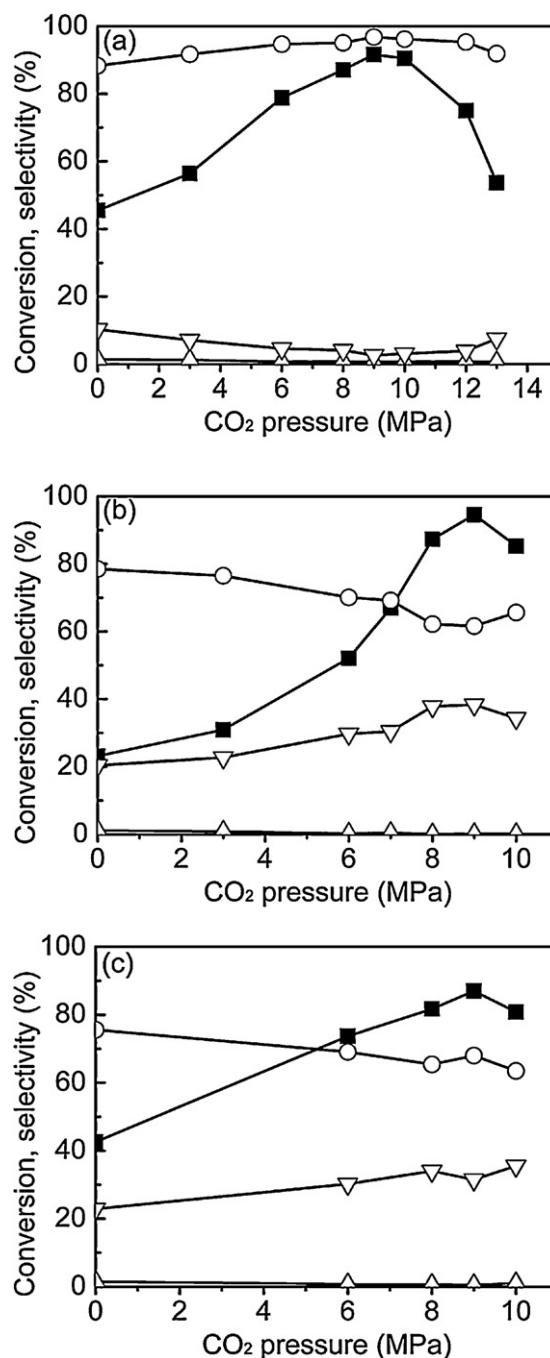


Fig. 1. Influence of CO₂ pressure on the conversion (■) and the selectivity for the hydrogenation of *o*-CNB. (a) 5% Pd/C in H₂O, (b) 5% Pt/C in H₂O, and (c) 5% Pt/C in pure CO₂. Reaction conditions: 1.5 g *o*-CNB, 5 mg catalyst, 4 MPa H₂, 10 ml H₂O, 35 °C, 50 min for 5% Pd/C and 15 min for 5% Pt/C. (○) *o*-CAN, (△) aniline and nitrobenzene, (▽) intermediates include *o*-chloronitrosobenzene, dichloroazoxybenzene, dichloroazobenzene, and dichlorohydrazobenzene.

two phases of gas (CO₂, H₂ and dissolved *o*-CNB) and liquid H₂O at pressure of CO₂ beyond 17.4 MPa were observed. The *o*-CNB volume was expanded with increasing of CO₂ pressure and the maximum volume was obtained at 9 MPa (Fig. 2b). A certain amount of *o*-CNB dissolved into the CO₂ phase with the further increasing of CO₂ pressure, and the *o*-CNB phase disappeared at 17.4 MPa (Fig. 2c). In the absence of H₂O, the *o*-CNB volume was expanded with increasing of CO₂ pressure and the maximum volume was also obtained at 9 MPa (Fig. 3b), however, a completely miscible mixture (*o*-CNB, H₂ and CO₂) was formed at 12.3 MPa CO₂ (Fig. 3c). In other words,

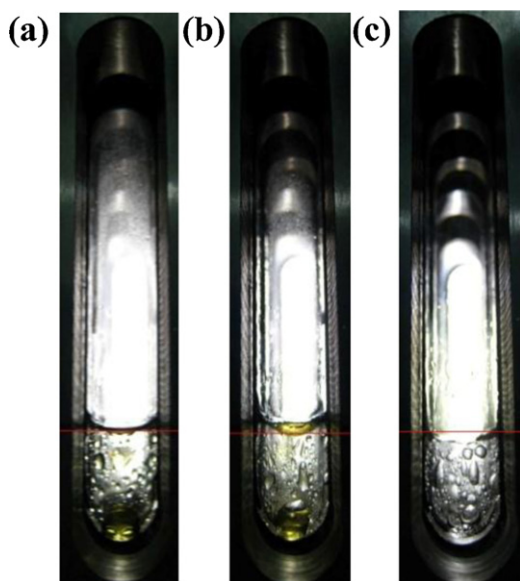


Fig. 2. Visual observations of the reaction mixture including *o*-CNB, H₂O, H₂, and CO₂ at 35 °C and at CO₂ pressures given (a) 0.1 MPa, (b) 9 MPa, (c) 17.4 MPa. Conditions: viewing cell volume 85 ml, 17 ml H₂O, 2.55 g *o*-CNB, 4 MPa H₂.

the higher CO₂ pressure was needed to dissolve *o*-CNB completely into CO₂ gas phase in the presence of H₂O, and this indicates the presence of interaction between H₂O and *o*-CNB.

Fig. 4 illustrates the processes for catalytic reaction and catalyst–product separation. Pd/C and Pt/C were hydrophobic catalysts and mainly disperse in *o*-CNB under stirring, the mass-transfer resistance between gas (H₂) and *o*-CNB droplet decreased with increasing of CO₂ pressure [38], so the reaction rate increased with CO₂ pressure in H₂O–CO₂ system. However, with the further increasing of CO₂ pressure, *o*-CNB was gradually extracted into scCO₂ phase, resulting in the decrease of *o*-CNB concentration in the liquid phase and the reaction rate decreased at pressure beyond 9 MPa CO₂. The maximum conversion was obtained at 9 MPa CO₂.



Fig. 3. Visual observations of the reaction mixture including *o*-CNB, H₂, and CO₂ at 35 °C and at CO₂ pressure given (a) 0.1 MPa, (b) 9 MPa, (c) 17.4 MPa. Conditions: viewing cell volume 74 ml, 2.22 g *o*-CNB, 4 MPa H₂.

for both Pd/C and Pt/C catalysts, and which increased 2 and 4 times compared to the value at 0.1 MPa CO₂ (Fig. 1a, b). In our previous work, however, the maximum conversion was obtained at 13 MPa CO₂ for Ni/TiO₂ catalyst at similar reaction conditions in H₂O–CO₂ system [29]. The maximum conversion presented at different CO₂ pressure was ascribed to the different properties of catalyst; Ni/TiO₂ catalyst is hydrophilic and mainly dispersed in water as shown in Fig. 5. *o*-CNB is partially soluble in CO₂ and CO₂ can partially soluble in H₂O [46], so the dissolution of CO₂ in H₂O can enhance the concentration of H₂ and *o*-CNB in H₂O phase and thus resulting in an enhancement of the reaction rate with increasing of CO₂ pressure. The maximum conversion presented at 13 MPa, at which the concentration of *o*-CNB in H₂O reached maximum. However, *o*-CNB could be gradually extracted into scCO₂ phase at the quite high pressure of CO₂ (>17.4 MPa), resulting in the decrease of *o*-CNB concentration in the aqueous phase, and so the reaction rate was decreased. But for the Pd/C and Pt/C catalysts, they are hydrophobic and mainly disperse in *o*-CNB phase (Fig. 4), with increasing of CO₂ pressure the CO₂ expanded liquid phase was formed (Fig. 2). The maximum conversion was obtained at 9 MPa in H₂O–CO₂ (Fig. 1b), at which the liquid phase was expanded maximum and the concentrations of H₂ and *o*-CNB in the liquid phase reached the largest value.

Moreover, the higher activity in H₂O–CO₂ can be explained by some factors. The acidic nature of the H₂O–CO₂ might be one of positive factors, but its effect is negligible [29]. The hydrogen bonding between water and the reacting species as described above may be an important factor. Interfacial hydrogen bonding of OH...ONO formed between H₂O and NB molecules [47], which may weaken the N–O bond. Previously, a striking rate increase was observed in some reactions on H₂O and this was ascribed to the hydrogen bonds between interfacial H₂O molecules and reactants or transition states [48]. In addition, our previous in situ FTIR showed that compressed CO₂ interacts with the reacting species, CNB, CNSB, and CPHA, decreasing the reactivity of CNB but increasing the reactivity of CNSB and CPHA [28]. These molecular interactions should also be important in the H₂O–CO₂–*o*-CNB reaction system.

The presence of CO₂ is helpful to suppress the dechlorination reactions of *o*-CNB and *o*-CAN over Pd/C and Pt/C in H₂O–CO₂. It was consistent with previous results [28,29,35,39] that CO generated from CO₂ hydrogenation could act as a modifier for Pt/C catalyst to block the active sites for dechlorination in scCO₂ [35].

3.3. Recycling of catalysts

The recycling of catalyst has been examined with Pd/C and Pt/C in H₂O–*n*-heptane and H₂O–CO₂ (Table 3). For Pd/C, the deactivation was obvious in H₂O–*n*-heptane and more serious in H₂O–CO₂. For Pt/C, the activity changed little in H₂O–*n*-heptane but decreased slightly in H₂O–CO₂, in these systems the similar selectivity was obtained after five recycles. ICP analysis was used to investigate the possibility of Pd and Pt leaching during the reaction in H₂O–*n*-heptane and H₂O–CO₂. Pd and Pt was not detected in filtrate due to the concentration was lower than the detection limit (0.1 ppm), it suggested that the leaching of Pd and Pt was negligible even though the H₂O–CO₂ reaction system presents somewhat acidity (ca. pH 3 [49]).

Since deactivation of supported catalysts usually relates with agglomeration of metal particles, the change of the particle sizes before and after reaction in H₂O–CO₂ was examined with XRD (Fig. 6). The average Pd and Pt particle sizes were 16.1 and 4.5 nm, respectively, and did not change after reaction. Therefore, the agglomeration of Pd and Pt particles were not the main factor to cause the deactivation of catalysts.

XPS was used to investigate the electronic state of Pd and Pt on the surface of the fresh and used catalysts. As shown in Fig. 7,

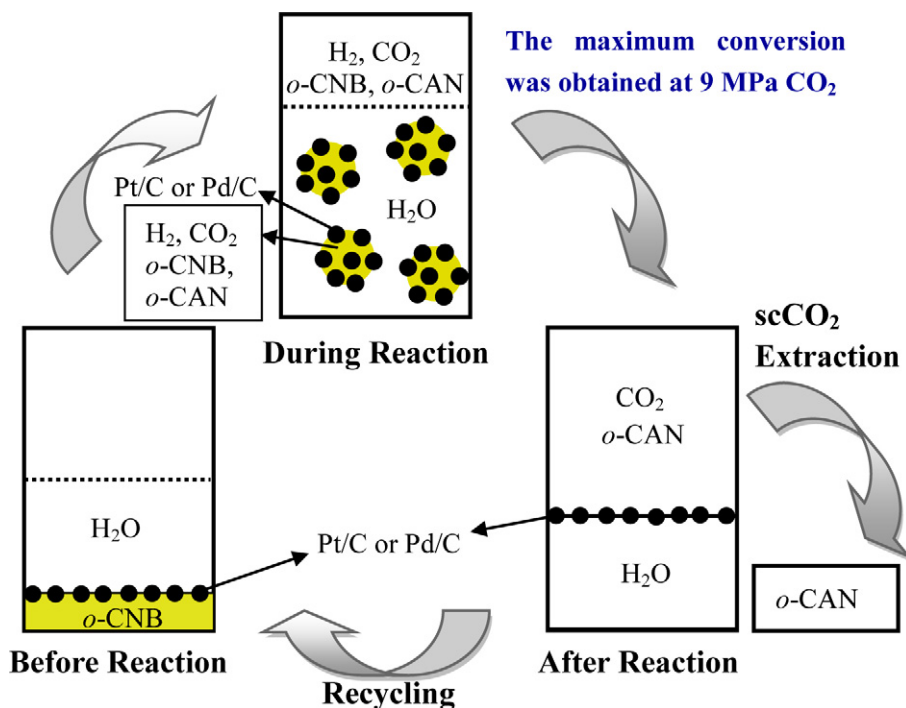


Fig. 4. Reaction, separation, and recycling processes for the hydrogenation of *o*-CNB over Pt/C or Pd/C catalyst under gas (H_2 , CO_2)–liquid (H_2O) conditions.

for Pd/C catalyst, the peaks with binding energy of Pd $3d_{3/2}$ at 340.3 eV and Pd $3d_{5/2}$ at 335.0 eV are characteristic of Pd⁰, and the peaks with binding energy of Pd $3d_{3/2}$ at 342.2 eV and Pd $3d_{5/2}$ at 337.0 eV are characteristic of Pd²⁺ [50]. The atomic ratios of Pd²⁺/Pd⁰ were 0.38 and 1.73 for the fresh and the used Pd/C catalysts in H_2O – CO_2 , respectively, indicating that the oxidization of Pd species was responsible for the deactivation of Pd/C during the hydrogenation of *o*-CNB. The oxidized Pd species may be amorphous, so no reflections associated with them were observed in

the XRD patterns of the Pd/C catalyst. For the fresh Pt/C catalyst, the peaks with binding energy of Pt $4f_{5/2}$ at 74.5 eV and Pt $4f_{7/2}$ at 71.0 eV are characteristic of Pt⁰. For the used Pt/C catalyst in H_2O – CO_2 , only two peaks corresponding to Pt⁰ were found, which are similar to the fresh catalyst; so Pt/C was much more stable than Pd/C in H_2O – CO_2 .

The deactivation of Pd/C catalyst was more serious in H_2O – CO_2 than that in H_2O –*n*-heptane (Table 3). The deactivation of Au/TiO₂ catalyst in the hydrogenation of *o*-CNB in the presence of CO_2 was

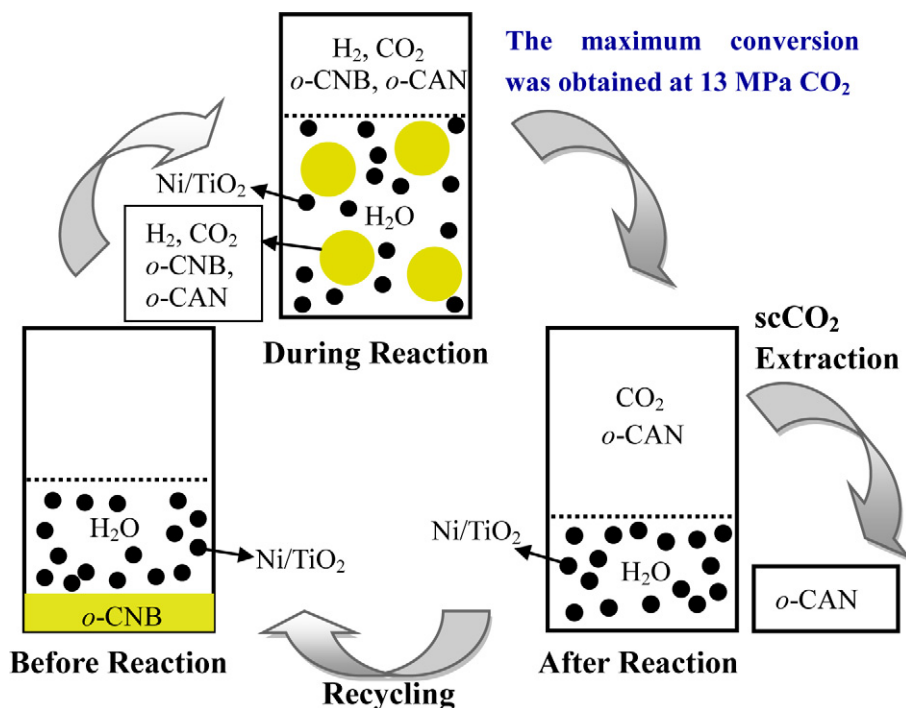


Fig. 5. Reaction, separation, and recycling processes for the hydrogenation of *o*-CNB over Ni/TiO₂ catalyst under gas (H_2 , CO_2)–liquid (H_2O) conditions.

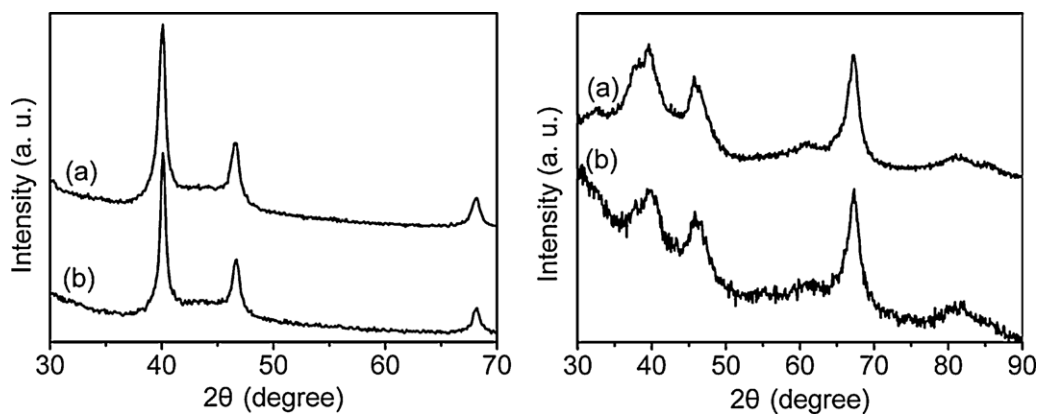


Fig. 6. XRD patterns of 5% Pd/C (left) and 5% Pt/C (right), (a) before reaction (b) after reaction in H₂O–CO₂.

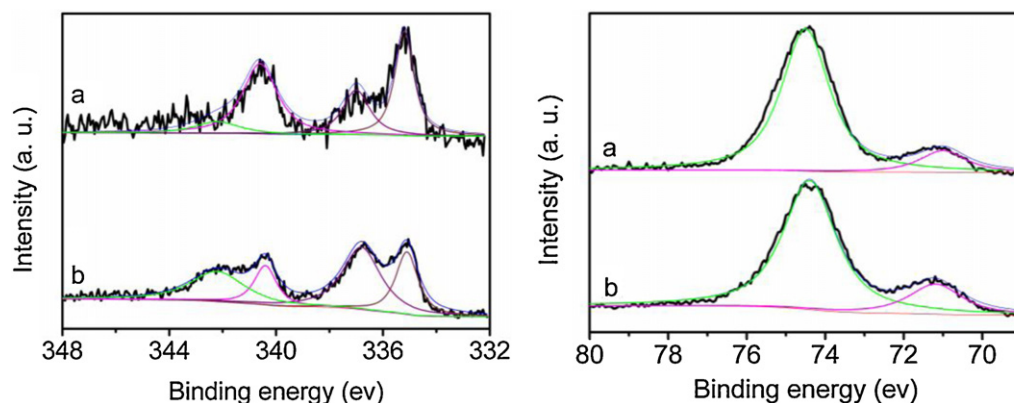


Fig. 7. XPS spectra of 5% Pd/C (left) and 5% Pt/C (right), (a) before reaction and (b) after reaction in H₂O–CO₂.

ascribed to the carbonate-like species forming on the surface of Au/TiO₂ and the original Au⁰ species partially oxidized by CO₂ [51]. Herein, the oxidation of Pd species was also presented in H₂O–CO₂, CO might be generated from CO₂ during the hydrogenation process and poisoned some active sites [35], and it may be

Table 3

Results of the catalyst recycling test in the hydrogenation of *o*-CNB over 5% Pd/C and 5% Pt/C in H₂O–*n*-heptane and H₂O–CO₂.

Catalyst	Run	Conversion (%)	Selectivity (%)		
			<i>o</i> -CAN	AN	Others
In H ₂ O– <i>n</i> -heptane					
Pd/C	1	98	98.9	0.5	0.6
	2	78	96.7	0.5	2.8
	3	58	95.9	0.9	3.2
Pt/C	1	90	89.5	0.3	10.2
	2	90	89.6	0.3	10.1
	3	91	89.6	0.2	10.2
	4	92	89.3	0.3	10.4
	5	91	84.3	0.3	15.4
In H ₂ O–CO ₂					
Pd/C	1	100	99.0	0.7	0.3
	2	30	83.5	2.9	13.6
	3	12	83.3	1.9	14.8
Pt/C	1	100	76.9	0.3	22.8
	2	99	80.9	0.2	18.9
	3	97	79.2	0.2	20.6
	4	93	84.1	0.2	15.7
	5	91	81.9	0.3	17.8

Reaction condition: 5 mg 5%Pd/C or 5% Pt/C, 9.52 mmol *o*-CNB, 4 MPa H₂, 35 °C. In H₂O–*n*-heptane: 2 ml H₂O, 10 ml *n*-heptane, 65 and 15 min of reaction over Pd/C and Pt/C, respectively. In H₂O–CO₂: 10 ml H₂O, 9 MPa CO₂, 65 and 25 min of reaction over Pd/C and Pt/C, respectively.

more serious for Pd/C. It is worth noting that the Pt/C, CO₂ and H₂O phase were easily separated from the organic product phase after the reaction. Hence, they are recyclable without any post purification, the H₂O–CO₂ and Pt/C catalyst system is effective for practical production of *o*-CAN from the hydrogenation of *o*-CNB.

4. Conclusions

The effects of water on the hydrogenation of *o*-CNB over Pt/C and Pd/C were studied in ethanol, *n*-heptane and compressed CO₂. The interactions of water with the reacting species and the solubility of hydrogen in liquid phase were considered to have largely influence to the reaction rate. The positive effect of interaction between H₂O and *o*-CNB by hydrogen bonding could counteract by the negative effect of hydrogen solubility in H₂O–ethanol resulting in a decrease in the TOF. While the concentrations of *o*-CNB and hydrogen changed very slightly in H₂O–*n*-heptane, so the molecular interaction played an important role in the improved TOF. Moreover, the higher TOF was obtained in H₂O–CO₂ system than that in H₂O and compressed CO₂ due to the phase behavior and the interactions among H₂O, CO₂ with CNB. In addition, the conversion over Pd/C and Pt/C in H₂O–CO₂ and pure scCO₂ presented the maximum values at 9 MPa, which is largely different to the results over previous Ni/TiO₂ (13 MPa). It was explained by the phase behavior and surface properties of Pd/C, Pt/C (hydrophobic) and Ni/TiO₂ (hydrophilic). The combination of H₂O and CO₂ is the most efficient and green reaction media for the present hydrogenation of CNB. However, the Pd/C catalyst deactivation was found, it deactivated faster in H₂O–CO₂ system compared to H₂O–*n*-heptane due to the changes of Pd species and the poisoning by CO generated during the reaction. Pt/C catalyst was stable in H₂O–*n*-heptane and

similar reaction rate and product selectivity was obtained after five times recycle, but it decreased slightly in H₂O–CO₂ system. The stability improvement of Pt/C catalyst will be further studied in our future work.

Acknowledgements

The authors gratefully acknowledge the financial supports from NSFC 21273222, 21202159 and 21143001, and from Jilin province, China 20100562.

References

- [1] S. Minakata, M. Komatsu, *Chem. Rev.* 109 (2009) 711–724.
- [2] A. Chanda, V.V. Fokin, *Chem. Rev.* 109 (2009) 725–748.
- [3] R.N. Butler, A.G. Coyne, *Chem. Rev.* 110 (2010) 6302–6337.
- [4] F. Joo, *Aqueous Organometallic Catalysis*, vol. 23, Kluwer Academic, Dordrecht, 2001.
- [5] V.V. Fokin, K.B. Sharpless, *Angew. Chem. Int. Ed.* 40 (2001) 3455–3457.
- [6] J. Morita, H. Nakatsuji, T. Misaki, Y. Tanabe, *Green Chem.* 7 (2005) 711–715.
- [7] J.C. Mao, B.S. Wan, F. Wu, S.W. Lu, *Tetrahedron Lett.* 46 (2005) 7341–7344.
- [8] X.L. Xu, T. Hirao, *J. Org. Chem.* 70 (2005) 8594–8596.
- [9] N. Jiang, A.J. Ragauskas, *Tetrahedron Lett.* 47 (2006) 197–200.
- [10] Y.Z. Xiang, L. Ma, C.S. Lu, Q.F. Zhang, X.N. Li, *Green Chem.* 10 (2008) 939–943.
- [11] Z.M. Wang, K.B. Sharpless, *J. Org. Chem.* 59 (1994) 8302–8303.
- [12] Z.P. Demko, K.B. Sharpless, *J. Org. Chem.* 66 (2001) 7945–7950.
- [13] S. Narayan, J. Muldoon, M.G. Finn, V.V. Fokin, H.C. Kolb, K.B. Sharpless, *Angew. Chem. Int. Ed.* 44 (2005) 3275–3279.
- [14] J.E. Klijn, J. Engberts, *Nature* 435 (2005) 746–747.
- [15] N. Shapiro, A. Vigalok, *Angew. Chem. Int. Ed.* 47 (2008) 2849–2852.
- [16] P. Maity, S. Basu, S. Bhaduri, G.K. Lahiri, *Adv. Synth. Catal.* 349 (2007) 1955–1962.
- [17] H.C. Yao, P.H. Emmett, *J. Am. Chem. Soc.* 81 (1959) 4125–4132.
- [18] H.C. Yao, P.H. Emmett, *J. Am. Chem. Soc.* 83 (1961) 796–799.
- [19] K. Taya, *Sci. Pap. I.P.C.R.* 56 (1962) 285–289.
- [20] S. Nishimura, *Handbook of heterogeneous catalytic hydrogenation for organic synthesis*, John Wiley & Sons, Inc., New York, 2001, 334.
- [21] J. Ning, J. Xu, J. Liu, H. Miao, H. Ma, C. Chen, X. Li, L. Zhou, W. Yu, *Catal. Commun.* 8 (2007) 1763–1766.
- [22] M. Pietrowski, M. Zielinski, M. Wojciechowska, *Catal. Lett.* 128 (2009) 31–35.
- [23] G.Y. Fan, L. Zhang, H.Y. Fu, M.L. Yuan, R.X. Li, H. Chen, X.J. Li, *Catal. Commun.* 11 (2010) 451–455.
- [24] R. Adams, F.L. Cohen, O.W. Rees, *J. Am. Chem. Soc.* 49 (1927) 1093–1099.
- [25] C.A. Eckert, B.L. Knutson, P.G. Debenedetti, *Nature* 383 (1996) 313–318.
- [26] T. Seki, J.D. Grunwaldt, A. Baiker, *Ind. Eng. Chem. Res.* 47 (2008) 4561–4585.
- [27] X.C. Meng, H.Y. Cheng, Y. Akiyama, Y.F. Hao, W.B. Qiao, Y.C. Yu, F.Y. Zhao, S. Fujita, M. Arai, *J. Catal.* 264 (2009) 1–10.
- [28] X.C. Meng, H.Y. Cheng, S. Fujita, Y.F. Hao, Y.J. Shang, Y.C. Yu, S.X. Cai, F.Y. Zhao, M. Arai, *J. Catal.* 269 (2010) 131–139.
- [29] X.C. Meng, H.Y. Cheng, S. Fujita, Y.C. Yu, F.Y. Zhao, M. Arai, *Green Chem.* 13 (2011) 570–572.
- [30] M. Chatterjee, A. Chatterjee, H. Kawanami, T. Ishizaka, T. Suzuki, A. Suzuki, *Adv. Synth. Catal.* 354 (2012) 2009–2018.
- [31] S. Fujita, X.C. Meng, F.Y. Zhao, M. Arai, in: M. R. Belinsky (Eds.), *Supercritical Fluids*. Nova Science Publishers, Inc., New York, 2010, p. 609–631.
- [32] S. Fujita, S. Akihara, F.Y. Zhao, R.X. Liu, M. Hasegawa, M. Arai, *J. Catal.* 236 (2005) 101–111.
- [33] C.M. Rayner, *Org. Process Res. Dev.* 11 (2007) 121–132.
- [34] F.Y. Zhao, S. Fujita, S. Akihara, M. Arai, *J. Phys. Chem. A* 109 (2005) 4419–4424.
- [35] S. Ichikawa, M. Tada, Y. Iwasawa, T. Ikariya, *Chem. Commun.* (2005) 924–926.
- [36] F. Zhao, Y. Ikushima, M. Arai, *J. Catal.* 224 (2004) 479–483.
- [37] F.Y. Zhao, S. Fujita, J.M. Sun, Y. Ikushima, M. Arai, *Catal. Today* 98 (2004) 523–528.
- [38] F.Y. Zhao, R. Zhang, M. Chatterjee, Y. Ikushima, M. Arai, *Adv. Synth. Catal.* 346 (2004) 661–668.
- [39] C.Y. Xi, H.Y. Cheng, J.M. Hao, S.X. Cai, F.Y. Zhao, *J. Mol. Catal. A: Chem.* 282 (2008) 80–84.
- [40] B.M. Bhanage, Y. Ikushima, M. Shirai, M. Arai, *Chem. Commun.* (1999) 1277–1278.
- [41] S. Fujita, S. Akihara, M. Arai, *J. Mol. Catal. A: Chem.* 249 (2006) 223–229.
- [42] H.W. Lin, C.H. Yen, C.S. Tan, *Green Chem.* 14 (2012) 682–687.
- [43] M. Jorge, M. Natalia, D.S. Cordeiro, *J. Phys. Chem. C* 111 (2007) 17612–17626.
- [44] G. Moakes, J. Janata, *Acc. Chem. Res.* 40 (2007) 720–728.
- [45] P. Politzer, J.S. Murray, M.C. Concha, *J. Phys. Org. Chem.* 21 (2008) 155–162.
- [46] L.W. Diamond, N.N. Akinfiev, *Fluid Phase Equilib.* 208 (2003) 265–290.
- [47] M. Jorge, M. Cordeiro, *J. Phys. Chem. C* 111 (2007) 17612–17626.
- [48] Y.S. Jung, R.A. Marcus, *J. Am. Chem. Soc.* 129 (2007) 5492–5502.
- [49] C. Roosen, M. Ansorge-Schumacher, T. Mang, W. Leitner, L. Greiner, *Green Chem.* 9 (2007) 455–458.
- [50] J.F. Moulder, W.F. Stickle, P.E. Sobol, K.D. Bomben, *Handbook of X-ray Photoelectron Spectroscopy: A Reference Book of Standard Spectra for Identification and Interpretation of Xps Data*, Perkin-Elmer, Physical Electronics Division, Eden Prairie, 1992.
- [51] Y.F. Hao, R.X. Liu, X.C. Meng, H.Y. Cheng, F.Y. Zhao, *J. Mol. Catal. A: Chem.* 335 (2011) 183–188.